Probability Distributions of Scalars in Turbulent Shear Flow

S. B. Pope

Massachusetts Institute of Technology, Department of Mechanical Engineering
Cambridge, MA 02139, USA

Abstract

A method of determining the statistically-mostlikely probability distribution of scalar quantities in turbulent flows has been described in previous works [2, 5]. The method is applicable to the joint probability density function (pdf) of any number of reactive or non-reactive scalars, and any number of moments can be incorporated. This paper reports, first, a comparison of most-likely pdf's with measured pdf's of passive scalars in turbulent shear flows. Secondly, the paper reports calculations of the evolution of the most-likely pdf of a reactive scalar in homogeneous turbulence. It is found that (with a single exception) the most-likely pdf based on the first three moments is in excellent quantitative agreement with the pdf's measured in shear flows. With only two moments, the most-likely pdf's are unable to adopt the sometimes-observed bimodal shapes. The calculations of reaction in homogeneous turbulence show that the pdf's are dominated by spikes at the two bounds. In addition it is found that, as the instantaneous reaction rate tends to infinity, the mean reaction rate tends to a universal function; this function is well represented by a simple empirical formula, Eq. (18).

Nomenclature

A_n	Coefficient in Eq. (1)
D	Jet diameter
H	Entropy (Eq. 7)
$p(\psi)$	Probability density function of ϕ
$\tilde{p}(\psi)$	Density-weighted pdf of ϕ
$q(\psi)$	*A priori* probability of ϕ
$Q(\psi)$	Arbitrary function
r	Radial distance
$S(\phi), S^*(\phi)$	Creation rate of ϕ, normalized creation rate
t, t^*	Time, normalized time
T, T_∞	Temperature, ambient temperature
$\underline{x}$	Position

Greek Symbols

α	Turbulent time scale/reaction time scale, Eq. (17)
Γ	Molecular diffusivity
λ	Number of moments
μ_n	nth central moment, $\mu_1 = \langle\phi\rangle$
ρ	Density
τ	Time scale Eq. (12)
$\phi, \langle\phi\rangle$	Scalar, mean of ϕ
ϕ'	Fluctuating or rms value of ϕ
ψ	Independent scalar variable

Introduction

Since the work of *Hawthorne* et al. [1], probability density functions have proved useful in the theoretical treatment of turbulent reacting flows. The representation of the pdf of a passive scalar as a function of its first and second moments has attracted much attention. Various authors have suggested a Gaussian, a beta-function distribution, a "clipped-Gaussian" and a double-delta function distribution (see [2] for references). In the model of *Bray* and *Moss* [3] a pdf for a single reactive scalar is prescribed and *Donaldson* and *Varma* [4] implicitly assume the joint pdf of reactive scalars to be comprised of delta functions. All these distributions are determined as functions of their first and second moments.

In previous work [2, 5] the author proposed a general method of determining single or joint pdf's of passive or reactive scalars in turbulent flows. The method is based on the assumption that the pdf is the statistically-most-likely distribution. An alternative view of this assumption can be based on the fact that the statistically-most-likely distribution contains a minimum of information. Consequently any other distribution contains more information, and the extra information is spurious. Thus, the assumption that the pdf is the statistically-most-likely distribution is the only assumption that excludes spurious information.

The method, which is described in the next section, is applicable to any number of scalars and any number of moments can be prescribed.

In the third section of the paper, the most-likely pdf's are compared with measurements made in turbulent shear flows. The data of *LaRue* and *Libby* [6] are of pdf's of temperature in the wake of a heated cylinder: the data of *Birch* et al. [7] are of pdf's of concentration in a turbulent methane jet in an atmosphere of air. Many of these pdf's are bimodal and, with a single exception, they are well represented by the most-likely distribution based on the first three moments. (Two moments are insufficient to describe bimodal distributions.)

Calculations of reaction in homogeneous turbulence are reported in the fourth section. These calculations are based on the solution of the differential equations for the mean and variance of a scalar which corresponds to the concentration of reaction products. An Arrhenius reaction rate is used and the mean reaction rate and rate correlations are determined from the assumption that the pdf adopts its most-likely value. The results show the evolution of the pdf which is dominated by spikes as the two bounds. For large reaction rates it is found that the mean reaction rate is a universal function for which an empirical formula is provided, Eq. (18).

Theory

In this section the results of previous work [2, 5] relevant to the present study are reported. If the first λ moments of the pdf $p(\psi)$ are known, then the most-likely value of p is

$$p_\lambda(\psi) \approx q(\psi) \exp\left(\sum_{n=0}^{\lambda} A_n \psi^n\right). \tag{1}$$

$q(\psi)$ is the *a priori* probability which, for nonreactive scalars, is a constant. $q(\psi)$ for a reactive scalar is given below, Eq. (8). The $\lambda + 1$ coefficients A in Eq. (1) are uniquely determined from the λ moments and from the condition that $p_\lambda(\psi)$ integrates to unity.

Let $\phi(\underline{x}, t)$ denote a scalar that obeys the conservation equation

$$\rho \frac{D\phi}{Dt} = \Gamma \nabla^2 \phi + \rho S(\phi), \tag{2}$$

where Γ is the molecular diffusivity and $S(\psi)$ is the rate of creation of ϕ. In a turbulent flow, the probability density function $p(\psi; \underline{x}, t)$ is defined so that the probability of ϕ being in the range $\psi < \phi < \psi + d\psi$ is $p(\psi)d\psi$. From this definition it follows that, if $Q(\phi)$ is any function, then its expected value (denoted by angled brackets) is

$$\langle Q[\phi(\underline{x}, t)]\rangle = \int p(\psi; \underline{x}, t) Q(\psi) d\psi. \tag{3}$$

By substituting, ψ and $(\psi - \langle\phi\rangle)^n$ for $Q(\psi)$ in Eq. (3), we obtain

$$\int p(\psi)d\psi = 1, \tag{4}$$

$$\int \psi p(\psi)d\psi = \langle\phi\rangle = \mu_1 \tag{5}$$

and

$$\int (\psi - \langle\phi\rangle)^n p(\psi)d\psi = \langle\phi'^n\rangle = \mu_n. \tag{6}$$

Thus, μ_1 is the mean of ϕ and $\mu_n (n > 1)$ is the nth central moment.

The most-likely pdf maximizes the entropy H subject to available information:

$$H \equiv -\int \ln [p(\psi)/q(\psi)] q(\psi) d\psi. \tag{7}$$

For a non-reactive scalar [$S(\phi) = 0$], the transport Eq. (2) is linear in ϕ: from this it follows that the *a priori* probability $q(\psi)$ is a constant (unity, say). For a single reactive scalar, the expression given by *Pope* [2] reduces to

$$q(\psi) = [1 + S(\psi)\tau/\phi'], \tag{8}$$

where ϕ' is the rms fluctuation ($\phi' = \mu_2^{1/2}$) and τ is the time scale of dissipation of ϕ' [see Eq. (12) below].

If the available information is the first λ moments of $p(\psi)$, then the calculus of variations can be used to show that the distribution that maximizes H is

$$p_\lambda(\psi) = q(\psi) \exp\left(\sum_{n=0}^{\lambda} A_n \psi^n\right). \tag{9}$$

The $(\lambda + 1)$ coefficients A are uniquely determined from the λ moments and from the condition that $p_\lambda(\psi)$ integrates to unity. The subscript λ indicates that $p_\lambda(\psi)$ is the most-likely distribution based on a knowledge of the first λ moments.

In the next section $p_\lambda(\psi)$ $(2 \leqslant \lambda \leqslant 5)$ is compared with experimental data of pdf's of a non-reactive scalar in shear flows. The moments μ_n were either taken directly from the data or were determined by numerical integration of the pdf. Then Eqs. (4–6) and (9) were solved using Newton's method in order to determine the coefficients A and hence $p_\lambda(\psi)$.

The penultimate section reports calculations of the evolution of $p_2(\psi, t)$ for a reaction in homogeneous turbulence. In those calculations the first two moments were determined from their conservation equations. For constant-density flow in homogeneous turbulence these are:

$$\frac{d\langle\phi\rangle}{dt} = \langle S(\phi)\rangle \tag{10}$$

and

$$\frac{1}{2}\frac{d\langle\phi'^2\rangle}{dt} = \langle\phi' S(\phi)\rangle - \left\langle \Gamma \frac{\partial\phi}{\partial x_i}\frac{\partial\phi}{\partial x_i}\right\rangle. \tag{11}$$

The last term in Eq. (11) accounts for the destruction of fluctuations of ϕ and it can be used to define the time scale of decay τ:

$$\tau = \langle\phi'^2\rangle / \left\langle \Gamma \frac{\partial\phi}{\partial x_i}\frac{\partial\phi}{\partial x_i}\right\rangle. \tag{12}$$

The time scale τ, which is presumed to be constant, is used to normalize t and $S(\phi)$:

$$t^* \equiv t/\tau \quad \text{and} \quad S^*(\phi) \equiv S(\phi)\tau. \tag{13}$$

Then, Eqs. (10) and (11) can be written,

$$\frac{d\langle\phi\rangle}{dt^*} = \langle S^*(\phi)\rangle \tag{14}$$

and

$$\frac{1}{2}\frac{d\langle\phi'^2\rangle}{dt^*} = \langle\phi' S^*(\phi)\rangle - \langle\phi'^2\rangle. \tag{15}$$

With the assumption that the pdf of ϕ is $p_2(\psi)$, $\langle S^*(\phi)\rangle$ and $\langle\phi' S^*(\phi)\rangle$ can be determined from, for example

$$\langle\phi' S^*(\phi)\rangle = \int (\psi - \langle\phi\rangle) S^*(\psi) p(\psi) d\psi. \tag{16}$$

Thus, with given initial conditions for $\langle\phi\rangle$ and $\langle\phi'^2\rangle$ and a given normalized rate of creation $S^*(\phi)$, Eqs. (14) and (15) can be integrated in normalized time. This integration was performed numerically to produce the results reported in the final section.

Comparison with Experiment

In this section the most-likely pdf's are compared with measurements of passive scalars in turbulent shear flows. The measurements of pdf's of temperature reported by *LaRue* and *Libby* [6] were obtained in the far wake of a heated cylinder; and the measurements of *Birch* et al. [7] are of pdf's of concentration in a methane jet.

Plane Wake

LaRue and *Libby*'s data were obtained at an axial distance of 400 diameters downstream of the cylinder. At this location, the maximum observed temperatures are well below the temperature of the cylinder. Consequently the only effective bound on the temperature is the

lower bound of the ambient temperature T_∞. The passive scalar is chosen to be $\phi \equiv T - T_\infty$, and hence $\phi \geqslant 0$.

Figures 1–5 show plots of $p(\psi)$ at increasing distances from the centre-line of the wake. The plots are normalized with the standard deviation of ϕ, ϕ'. The measured values of the moments were used to determine the most-likely pdf's based on the first two and three moments, $p_2(\psi)$ and $p_3(\psi)$. These are shown as dashed and full lines, respectively, and the experimental data are shown as circles.

Close to the centre-line (Figs. 1 and 2) the pdf's have a Gaussian shape except at the lower bound $\psi = 0$. However, the most-likely pdf based on the first two moments $p_2(\psi)$ does not follow the data; $p_3(\psi)$ does. Further away from the wake centre-line (Figs. 3–5) the pdf's become bimodal. Since $p_2(\psi)$ does not have sufficient degrees of freedom to adopt such a shape, it provides a poor representation of the measured pdf. On the other hand, the most-likely distribution based on three moments still follows the data closely. Indeed, at all five locations, discrepancies between $p_3(\psi)$ and the data are most likely less than experimental error.

From this comparison it can be concluded that, with a knowledge of only two moments, the most-likely distribution has a different shape from that measured. With a knowledge of three moments, not only is the shape correct, but also the quantitative agreement is excellent – at least for this flow.

Axisymmetric Jet

Birch et al. used laser Raman spectroscopy to measure the pdf of concentration ten nozzle diameters downstream of the exit of a methane jet. In this case the passive scalar ϕ is taken simply as the methane concentration: $\psi = 1$ corresponds to pure methane and $\psi = 0$ to pure air.

For variable-density flows ($\rho_{\text{methane}} \approx 0.55\ \rho_{\text{air}}$) it has been argued [8, 2] that it is appropriate to consider density-weighted quantities. The density-weighted pdf $\tilde{p}(\psi)$ is given by the relation

$$\langle\rho\rangle\tilde{p}(\psi) = \rho(\psi)p(\psi).$$

This relation was employed to determine $\tilde{p}(\psi)$ from *Birch* et al.'s measurements of $p(\psi)$, and the density-weighted moments were obtained by numerical integration of $\tilde{p}(\psi)$.

Figures 6–9 show $\tilde{p}_2(\psi)$ and $\tilde{p}_3(\psi)$ compared with the measurements at increasing distances from the jet axis. As before, near the axis (Figs. 6 and 7) the pdf's are Gaussian shaped but $\tilde{p}_2(\psi)$ is evidently discrepant. The curve of $\tilde{p}_3(\psi)$ passes through the data points. At $r/D = 1.49$ (Fig. 8) the measured pdf is bimodal and the shape appears to be similar to that of *LaRue* and *Libby*'s data. However, since neither $\tilde{p}_2(\psi)$ nor $\tilde{p}_3(\psi)$ are bimodal they provide poor representations of the measured pdf. Why this is so is discussed further below, but a clear answer is not evident. At the furthest radius measured (Fig. 9), the distribution ceases to be bimodal and is well represented by $\tilde{p}_3(\psi)$. As before, there is a noticeable difference between $\tilde{p}_2(\psi)$ and the data.

The distribution at $r/D = 1.49$ (Fig. 8) was investigated further. Figure 10 shows the data compared with the most-likely distributions based on four and five moments, $\tilde{p}_4(\psi)$ and $\tilde{p}_5(\psi)$. It may be seen that $\tilde{p}_4(\psi)$ is bimodal but a quantitative discrepancy remains. On the other hand, the curve of $\tilde{p}_5(\psi)$ passes through the data points. This confirms that with sufficient moments the most-likely distribution fits the data, but a five-parameter fit to fifteen data points can be expected to succeed.

Figs. 1–5. Comparison of most-likely distributions with data of *LaRue* and *Libby* [6]. Axial distance $x = 400\,d$: radial distance y is normalized with $l_c = (x - x_0)^{1/2} d^{1/2}$, where the virtual origin $x_0 = -40\,d$.

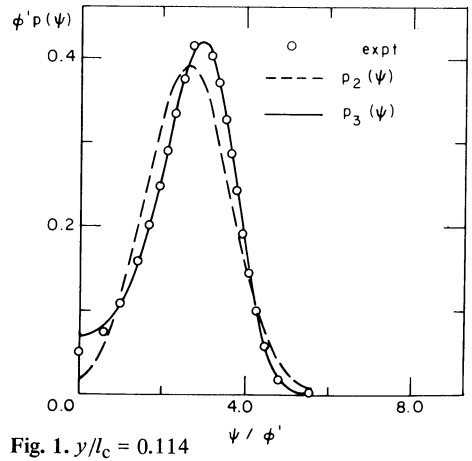

Fig. 1. $y/l_c = 0.114$

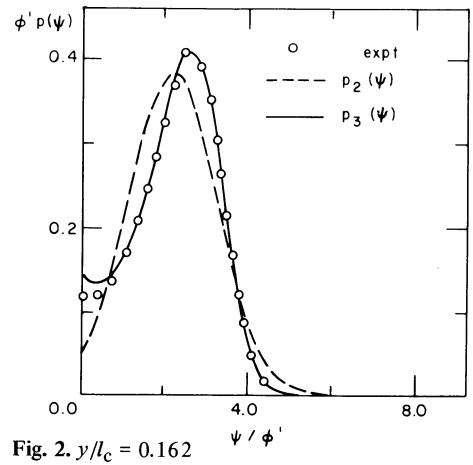

Fig. 2. $y/l_c = 0.162$

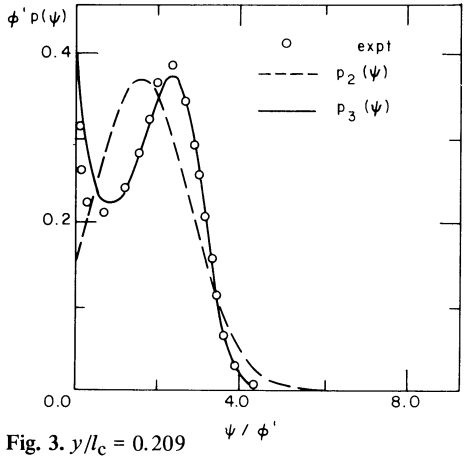

Fig. 3. $y/l_c = 0.209$

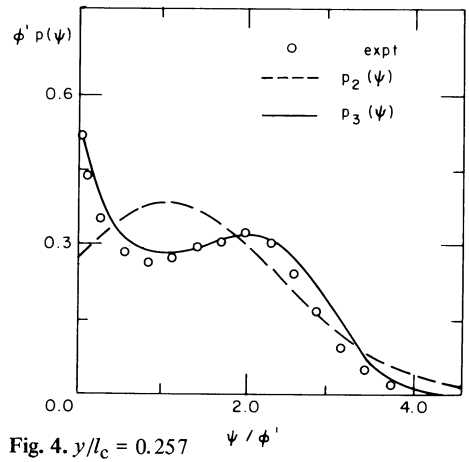

Fig. 4. $y/l_c = 0.257$

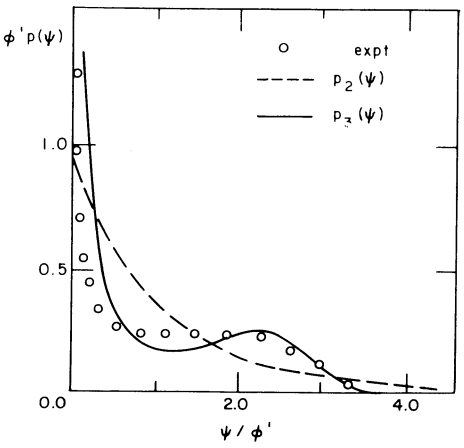

Fig. 5. $y/l_c = 0.294$

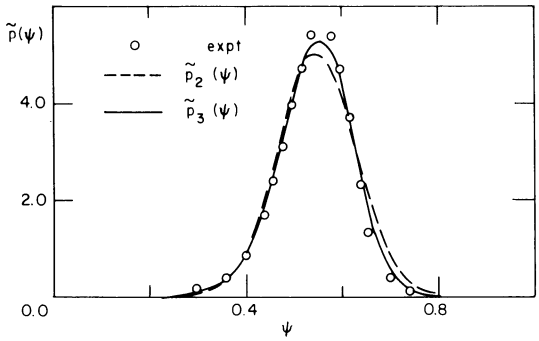

Fig. 6. $r/d = 0.0$

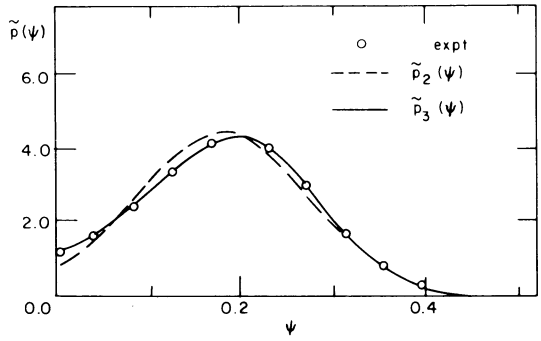

Fig. 7. $r/d = 1.3$

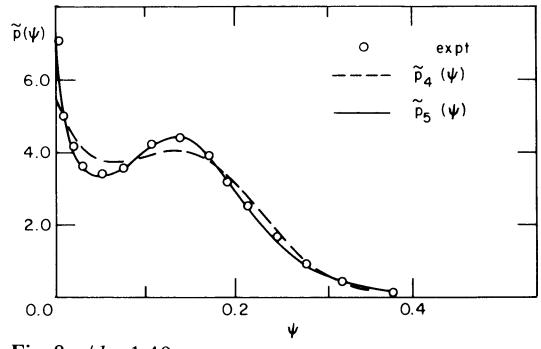

Fig. 8. $r/d = 1.49$

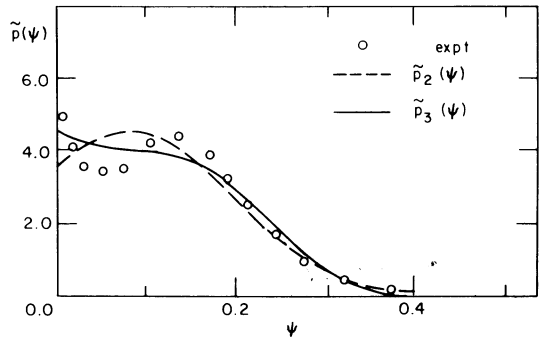

Fig. 9. $r/d = 1.8$

Figs. 6–10. Comparison of most-likely distributions with the data of *Birch* et al. [7]. Axial distance $x = 10\,d$.

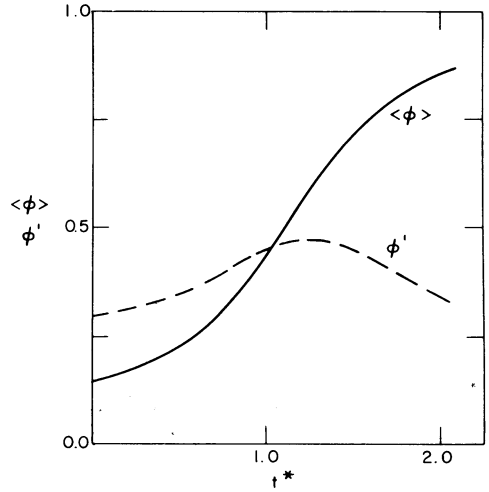

Fig. 10. $\langle\phi\rangle$ and ϕ' against t^* for $\alpha = 5$

Table 1. Skewness of distributions, data of [7]

	Skewness at $r/D = 1.3$	
	Weighted	Unweighted
Experimental	0.0572	0.0865
Most-likely distribution	0.2330	0.2620
Difference	−0.1758	−0.1755
	Skewness at $r/D = 1.49$	
	Weighted	Unweighted
Experimental	0.468	0.508
Most-likely distribution	0.690	0.741
Difference	0.222	0.233

Perhaps, contrary to the opinion expressed above, the unweighted pdf $p(\psi)$ should be considered rather than the density-weighted pdf $\tilde{p}(\psi)$. In order to investigate this question, the skewness of $p_2(\psi)$ and $\tilde{p}_2(\psi)$ were compared with the experimental values for $r/D = 1.3$ and $r/D = 1.49$. The results are shown in Table 1.

The difference between the experimental skewness and that given by $p_2(\psi)$ and $\tilde{p}_2(\psi)$ is a measure of the disagreement. It may be seen that, at both locations, the disagreement is nearly the same for weighted and unweighted pdf's. Consequently, the use of density-weighted pdf's cannot be deemed the cause of the observed discrepancy at $r/D = 1.49$.

In summary, for both the plane wake and the axisymmetric jet, in general there is excellent agreement between experimental data and the most-likely distribution based on three moments. The significant disagreement in one case remains unexplained. With only two moments prescribed, the most-likely distribution does not adopt observed bimodal shapes. Even where the pdf is not bimodal, there are discernible quantitative differences between $p_2(\psi)$ and the data.

Reaction in Homogeneous Turbulence

The evolution of the pdf of a reactive scalar in homogeneous turbulence was calculated by numerical integration of Eqs. (14) and (15) for $\langle\phi\rangle$ and ϕ' with the assumption that $p(\psi)$ is the most-likely distribution $p_2(\psi)$. The scalar ϕ is taken to represent the mass fraction of combustion products – $\psi = 0$ and $\psi = 1$ corresponding, respectively, to unburnt and fully burnt mixtures. Reaction proceeds according to the Arrhenius expression

$$S^*(\phi) = \alpha\, 6.11 \times 10^7\, \phi(1-\phi) \exp\left[-30{,}000/(300 + 1{,}800\,\phi)\right]. \tag{17}$$

The parameter α can be regarded as the ratio of the turbulent time scale to the reaction time scale. The multiplier 6.11×10^7 is chosen so that the maximum value of $S^*(\phi)$ is α: this maximum value occurs at $\phi = 0.933$.

For all the calculations reported, the initial conditions correspond, approximately, to the pdf $p_2(\psi)$ being a double-delta function distribution. The initial value of $\langle\phi\rangle$ is chosen so that reaction starts and continues at a reasonable rate.

Figure 10 shows the mean $\langle\phi\rangle$ and standard deviation ϕ' as a function of the normalized time t^*, for $\alpha = 5$. The mean increases monotonically (as it must) whereas ϕ' increases to a maximum of 0.47 before decaying. Since diffusion tends to decrease ϕ', the observed rise in ϕ' is due to reaction.

Figure 11 shows three pdf's taken from the same calculation (i.e. $\alpha = 5$). The arrows on the figure indicate the values of $\langle\phi\rangle$ for each pdf: these are $\langle\phi\rangle = 0.3$, 0.5 and 0.7. It may be seen that for each pdf there are spikes at zero and one with a relatively low value of $p(\psi)$ in between. This shape is precisely the one assumed in the models of *Bray* and *Moss* [3] and *Pope* [8]. The width of the spike at zero decreases as time (and hence $\langle\phi\rangle$) increases. The behaviour of the two spikes is more clearly seen on Fig. 12 where $p(0)$ and $p(1)$ are plotted against $\langle\phi\rangle$. The value at the upper bound $p(1)$ increases rapidly from its initial value of 15 to well over 100. The value at the lower bound $p(0)$ first falls, then rises to a maximum, and then falls again, ultimately to zero. In fact it can be shown from the pdf transport equation [10] that $p(0)$ must decrease monotonically. Ironically, the slight increase shown on Fig. 12 represents a violation of the second law.

It is generally held that as the instantaneous reaction rate $S(\phi)$ becomes large (compared with the turbulent frequency $1/\tau$) the mean reaction rate $\langle S(\phi)\rangle$ becomes independent of $S(\phi)$. In the present notation this implies that $\langle S^*(\phi)\rangle$ is independent of α for large α. This tenent

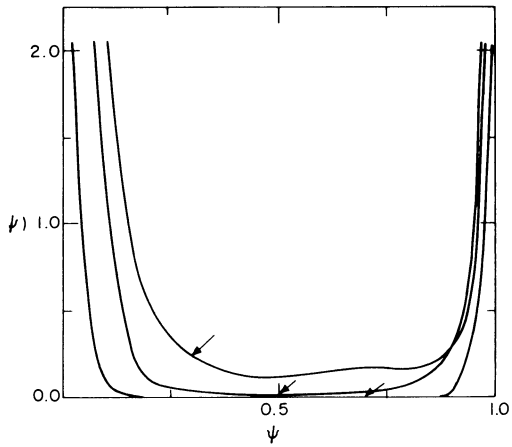

Fig. 11. $p(\psi)$ against ψ for $\alpha = 5$: $\langle\phi\rangle = 0.3$, 0.5 and 0.7

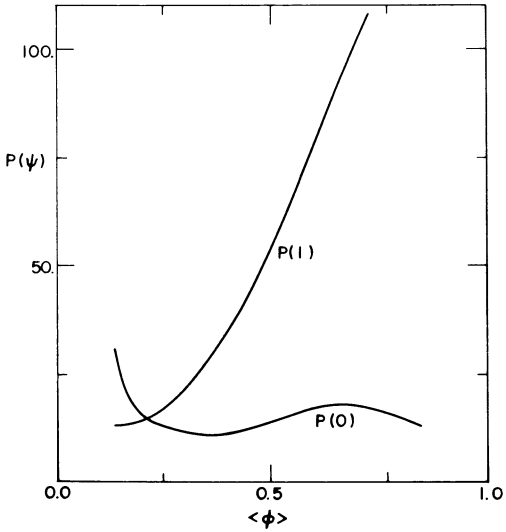

Fig. 12. $p(0)$ and $p(1)$ against $\langle\phi\rangle$ for $\alpha = 5$

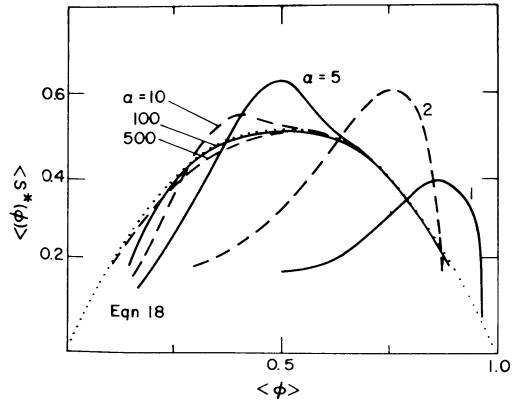

◀ **Fig. 13.** $\langle S^*(\phi)\rangle$ against $\langle\phi\rangle$ for $\alpha = 1$, 2, 5, 10, 100 and 500. The dotted line is Eq. (18)

was investigated by integrating equation (14) and (15) for various values of α: the computed values of $\langle S^*(\phi)\rangle$ are plotted against $\langle\phi\rangle$ on Fig. 13.

For the smallest instantaneous reaction rate ($\alpha = 1$), the reaction cannot be sustained unless the initial value of $\langle\phi\rangle$ is greater than 0.5. Then the mean reaction rate starts at a value of 0.2, rises to 0.4 at $\langle\phi\rangle = 0.85$ and then falls rapidly. For the next two values of α (2 and 5) the same trend is observed but the higher maximum of $\langle S^*(\phi)\rangle = 0.6$ is reached sooner (at $\langle\phi\rangle = 0.7$ and 0.5 respectively). For these three cases $\langle S^*(\phi)\rangle$ is clearly a strong function of α. The independence of $\langle S^*(\phi)\rangle$ from α becomes evident for the larger values, $\alpha = 10$, 100 and 500. Although the three curves differ slightly where $\langle\phi\rangle$ is less than 0.5, over the other half of the range the three curves coincide. The curve for $\alpha = 5$ also joins this apparently universal curve at $\langle\phi\rangle = 0.7$.

The existence of a universal curve of $\langle S^*(\phi)\rangle$ against $\langle\phi\rangle$ supports the tenent that the mean reaction rate becomes independent of $S(\phi)$ for large $S(\phi)$. In addition, the universal relationship between $\langle S^*(\phi)\rangle$ and $\langle\phi\rangle$ can be used as a model of premixed turbulent combustion. It is fortunate then that the simple empirical formula

$$\langle S^*(\phi)\rangle = 2.2\,\langle\phi\rangle\,(1 - \langle\phi\rangle) \tag{18}$$

provides an excellent representation of the curve (see the dotted line on Fig. 13).

To conclude: for reaction in homogeneous turbulence, the differential equations for $\langle\phi\rangle$ and $\langle\phi'^2\rangle$ are closed by the assumption that $p(\psi)$ adopts its most-likely value. These equations have been solved numerically to produce the results reported in this section. The results confirm the expectations that the pdf is approximately a double-delta function distribution, and that the mean reaction rate becomes independent of the instantaneous rate. Equation (18) provides an empirical formula for the mean reaction rate $\langle S^*(\phi)\rangle$ which is in excellent agreement with the calculated dependence of $\langle S^*(\phi)\rangle$ upon $\langle\phi\rangle$.

References

1. W. R. Hawthorne, D. S. Wedell, H. C. Hottel: Third Symposium (International) on Combustion (1949) pp. 266–288
2. S. B. Pope: The statistical theory of turbulent flames. Philos. Trans. R. Soc. London Ser. A **291**, 529 (1979)
3. K. N. C. Bray, J. B. Moss: AASU Rpt. 335, University of Southampton (1974)
4. C. du P. Donaldson, K. A. Varma: Combust. Sci. Tech. **13**, 55–73 (1976)
5. S. B. Pope: A rational method of determining probability distributions in turbulent reacting flows. J. Non-Equilib. Thermodyn. **4**, 309 (1979)
6. J. C. LaRue, P. A. Libby: Phys. Fluids **17**, 1956 (1974)
7. A. D. Birch, D. R. Brown, M. G. Dodson, J. R. Thomas; "Studies of Flammability in Turbulent Flows Using Laser Raman Spectroscopy". 17th Symposium (International) on Combustion, The Combustion Institute (1979)
8. R. W. Bilger: Combust. Sci. Tech. **11**, 215 (1975)
9. S. B. Pope: Combust. Flame **29**, 235 (1977)
10. S. B. Pope: Combust. Flame **27**, 299 (1976)